Atmos. Chem. Phys. Discuss., 9, 10303–10336, 2009
www.atmos-chem-phys-discuss.net/9/10303/2009/

Atmospheric Chemistry and Physics Discussions

This discussion paper is/has been under review for the journal *Atmospheric Chemistry and Physics (ACP)*. Please refer to the corresponding final paper in *ACP* if available.

Cloud condensation nuclei measurements in the eastern Mediterranean marine boundary layer: CCN closure and droplet growth kinetics

A. Bougiatioti[1], C. Fountoukis[3,4], N. Kalivitis[1], S. N. Pandis[4,5], A. Nenes[2,3], and N. Mihalopoulos[1]

[1]Environmental Chemical Processes Laboratory, Department of Chemistry, University of Crete, Voutes, 71003, Heraklion, Greece
[2]Earth and Atmospheric Sciences, Georgia Institute of Technology, Atlanta, GA 30332, USA
[3]Chemical and Biomolecular Engineering, Georgia Institute of Technology, Atlanta, GA 30332, USA

[4] Institute of Chemical Engineering and High Temperature Chemical Processes (ICE-HT), Foundation for Research and Technology Hellas (FORTH), Patras, 26504, Greece
[5] Department of Chemical Engineering, Carnegie Mellon Univ., Pittsburgh, PA 15213, USA

Received: 10 March 2009 – Accepted: 6 April 2009 – Published: 27 April 2009

Correspondence to: N. Mihalopoulos (mihalo@chemistry.uoc.gr)

Published by Copernicus Publications on behalf of the European Geosciences Union.

Abstract

Measurements of cloud condensation nuclei (CCN) concentrations (cm^{-3}) between 0.2 and 1.0% supersaturation, aerosol size distribution and chemical composition were performed at a remote marine site in the eastern Mediterranean, from September to October 2007 during the FAME-07 campaign. Virtually all the particles activate at 0.8% supersaturation, consistent with the very aged nature of the aerosol sampled. Application of Köhler theory, using measurements of bulk composition and size distribution, and assuming that organics are insoluble resulted in agreement between predicted and measured CCN concentrations within 3.4±11% for all supersaturations, with a tendency for CCN underprediction (15±8%; r^2=0.92) at lower supersaturations (0.2-0.4%). Including the effects of the water-soluble organic fraction (which represents around 70% of the total organic content) reduces the underprediction bias at low supersaturations, but introduces a slight overprediction (around 5±15%) bias at higher supersaturations (0.6–0.8%), likely from size-dependent variations of the sulfate to organic ratio. Using threshold droplet growth analysis, the growth kinetics of ambient CCN is consistent with NaCl calibration experiments; hence the presence of aged organics does not suppress the rate of water uptake in this environment. The knowledge of the soluble fraction is sufficient for the description of the CCN activity in this area.

1 Introduction

The absorption and scattering of radiation by atmospheric aerosol particles, especially those from anthropogenic activities, is an important component of anthropogenic climate change (IPCC, 2007). Aerosol particles also act as cloud condensation nuclei (CCN) and "indirectly" force climate through modification of cloud radiative properties and precipitation efficiency (Twomey, 1977; Albrect, 1989). Of all components of anthropogenic climate change, the aerosol indirect effect is the most uncertain (IPCC, 2007). Therefore, the ability to predict the CCN activity of ambient atmospheric aerosol

ACPD
9, 10303–10336, 2009

is required for predictive understanding of aerosol impacts on the Earth's climate.

The main physical-chemical principles involved in the transformation ("activation") of CCN into a cloud droplet involve the effects of curvature and solute on the equilibrium water vapor pressure. The simplest form of this theory, introduced by Köhler in the early 20th century (Köhler, 1921, 1936) was initially developed to describe the activation of marine (NaCl) aerosol particles. With appropriate extensions to account for the multicomponent nature of global aerosol, Köhler theory remains the theoretical basis for linking aerosol to CCN activity, as it determines the characteristic (or "critical") level of ambient water vapor supersaturation, S_c, required for particles to activate into cloud droplets. For a given aerosol particle, S_c depends on the particle dry size and chemical composition. For an aerosol size distribution of known chemical composition, the number concentration of CCN as a function of ambient supersaturation (the "CCN spectrum") can then be computed and used in physically-based parameterizations of cloud droplet activation (e.g., Nenes et al., 2003; Fountoukis and Nenes, 2005; Barahona and Nenes, 2007).

The ultimate test of Köhler theory is a "CCN closure" study, where measured CCN spectra are compared against predictions from measurements of aerosol chemical composition and size distribution. A successful closure study is when these two quantities are comparable within measurement uncertainty.

CCN closure studies have been underway many years with varying degrees of success. Liu et al. (1996) measured CCN at Chebogue Point in 1993 during the North Atlantic Regional Experiment (NARE) intensive. With a DH Associates static-diffusion cloud chamber operating at 0.4% supersaturation, size distribution from a PMS passive cavity aerosol spectrometer probe and chemical composition from filter samples, closure was achieved for 75% of the time. Covert et al. (1998) measured CCN concentrations with a static-diffusion cloud chamber at 0.5% supersaturation, and aerosol size distributions with a differential mobility particle sizer during the First Aerosol Characterization Experiment at Cape Grim, Tasmania, 1995. On average, closure was obtained with a slight tendency for overprediction (20%). Cantrell et al. (2001) mea-

sured CCN at the Kaashidhoo Climate Observatory during the Indian Ocean Experiment (INDOEX, 1999), using an aerosol time-of-flight spectrometer for the chemical composition and four micro-orifice uniform deposit cascade impactors (MOUDIs). Size distributions were measured using a TSI SMPS and CCN spectra were obtained using a CCN Remover (Ji et al., 1998), resulting in closure in 8 out of 10 cases, with discrepancies increasing with organic mass fraction. Roberts et al. (2003) performed CCN measurements during the Cooperative LBA (Large-scale Biosphere-Atmosphere Experiment in Amazonia, 1998) using a static diffusion cloud chamber between 0.15 and 1.5% supersaturation, a scanning mobility particle sizer for size distribution and a multistage cascade impactor for chemical composition, concluding that the CCN activity of aerosol in the LBA strongly depended on the water-soluble fraction. During the ACE-2 campaign, Snider et al. (2003) and Dusek et al. (2003) both performed CCN closure studies. Snider et al. (2003) attained closure for 2 out of 5 study days, unaffected by continental pollution. Dusek et al. (2003) overestimated calculated CCN on average by 30%, despite neglecting the effect of WSOC constituents on CCN activity.

VanReken et al. (2003) performed airborne CCN measurements during the Cirrus Regional Study of Tropical Anvils and Cirrus Layers-Florida Area Cirrus Experiment (CRYSTAL-FACE 2002) using two continuous-flow streamwise temperature gradient chambers (Roberts and Nenes, 2005), at 0.2 and 0.85% supersaturations. Closure was achieved within 5% at 0.2% supersaturation and 9% at 0.85% supersaturation. Using similar instrumentation, Rissman et al. (2006) performed an inverse aerosol-CCN closure, during the 2003 DOE-ARM intensive at the Southern Great Plains site (Oklahoma). Optimum closure was obtained when the population of aerosol was treated as an external mixture of particles, with the insoluble constituents preferentially distributed in particles less than 50 nm diameter. Broekhuizen et al. (2006) attained closure within 4% (on average), measuring CCN with a continuous thermal-gradient diffusion chamber at 0.58% for 4 days in Toronto, along with a TSI SMPS and an Aerodyne aerosol mass spectrometer for the size-dependent composition.

During the Chemical Emissions, Loss, Transformation and Interactions with

ACPD
9, 10303–10336, 2009

Canopies (CELTIC) field program at Duke Forest in North Carolina, Stroud et al. (2006) measured aerosol size-distribution with a TSI SMPS, chemical composition with an AMS and CCN concentrations with a static-diffusion cloud chamber. CCN predictions were within a factor of two of the observations. Ervens et al. (2007) measured the number concentration of CCN at five supersaturations (0.07 to 0.5%) during the International Consortium for Atmospheric Research on Transport and Transformation (ICARTT) field experiment at Chebogue Point (2004). CCN concentrations were predicted using measured size distributions, a simple aerosol model to derive the solute-to-water mole ratio, and the diameter growth factor or the optical growth factor. The mean error ranged from an overestimate of ≤5% at high supersaturation to a factor of 2.4 at low supersaturation. During the same campaign (ICARTT 2004), Medina et al. (2007) measured CCN at the UNH-AIRMAP Thompson Farms site, using a DMT streamwise thermal-gradient CCN counter (Roberts and Nenes, 2005), an AMS for size distribution of chemical composition and a TSI SMPS. Using "simple" Köhler theory and size-averaged chemical composition, CCN were substantially overpredicted (by 35.8±28.5%) and by introducing size-dependent chemical composition the closure was improved considerably (average error 17.4±27%).

The aforementioned studies are representative but by no means complete subset of the published CCN closure literature; all point out that in many cases Köhler theory sufficiently describes the activation of ambient aerosol, provided that the chemical composition, aerosol size distribution and mixing state are well constrainted. CCN prediction error most often arises from sampling or instrumentation limitations, especially when determining the aerosol chemical composition. The latter is quite important if the aerosol is externally mixed, or contains a large fraction of organic compounds. However, the treatment of organics in Köhler theory remains challenging and may explain some of the observed discrepancies in previous studies. A comprehensive application of Köhler theory, that accounts for the effects of the water-soluble organic carbon (WSOC) fraction of the aerosol is challenging for a number of reasons. WSOC can act as a surfactant, lowering droplet surface tension (Facchini et al.,1999; Decesari et al.,

ACPD
9, 10303–10336, 2009

2003) and may also contribute solute (Shulman et al., 1996), although the presence of soluble inorganic salts can diminish its importance (e.g., Ervens et al., 2007). The insoluble fraction of organics may also affect the uptake rate of water (e.g., Asa-Awuku et al., 2009) with important implications for cloud droplet number (e.g., Nenes et al., 2002). Since each of these effects alone can either enhance or diminish the CCN activity and droplet number in ambient clouds, the interpretation of the role of organics on CCN activation may be quite complex, and requires observational constraints to express their importance.

In the present paper, we report the CCN concentrations and the activation characteristics of atmospheric aerosols in a diversity of air masses sampled at an Eastern Mediterranean ground site during the Finokalia Aerosol Measurement Experiment-2007 (FAME-07) campaign. The present study is the first to report data of CCN measurements in the area, and complements existing studies on the aerosol characteristics in this climatically sensitive area of the globe (Lelieveld et al., 2002; Vrekoussis et al., 2005). In the following sections, CCN closure studies are carried out, with the goal of testing the applicability of "simple" Köhler theory for the prediction of CCN concentrations in a remote area with aged aerosol. The contribution of the aerosol organic fraction to CCN activity is also assessed, as well as its potential impact on droplet growth kinetics.

2 Observational data set

2.1 Measurement site

The Finokalia station (35°32′ N, 25°67′ E; http://finokalia.chemistry.uoc.gr) is a remote marine background site (50 m from the shore and 230 m above sea level) established and operated by the University of Crete. A detailed description of the site and prevailing meteorology can be found in Mihalopoulos et al. (1997) and Sciare et al. (2003). Finokalia is located at a unique "crossroad" of aged aerosol types, which

ACPD
9, 10303–10336, 2009

can originate from the marine boundary layer, Saharan desert, European subcontinent, and, biomass burning events during the summer period. The measurements presented in this study were obtained from mid-June to mid-October 2007, during the FAME-07 campaign, focused on understanding the properties of regional aged aerosol and their effects on regional climate. Analysis of HYSPLIT backtrajectories (www.arl.noaa.gov/ready/hysplit4.html) are then used to correlate measured aerosol properties with air mass origin. Throughout the campaign, both "polluted" air masses from Europe, the former Soviet Union and Asia Minor (Fig. 1a, b) and "cleaner" air masses from the Mediterranean and North Africa (Fig. 1c, d) were sampled.

2.2 Instrumentation setup

The instrumentation setup consisted of a Droplet Measurement Technologies (DMT) streamwise thermal-gradient CCN counter (Roberts and Nenes, 2005), a scanning mobility particle sizer (SMPS TSI 3080; composed of a TSI 3010 condensation particle counter and a TSI 3081L differential mobility analyzer) was used to measure the dry aerosol size distribution. The bulk (PM_1, $PM_{2.5}$) aerosol chemical composition was concurrently measured, using 4-h filter samples that were continuously collected during the campaign. Auxiliary chemical measurements (O_3, NO_x, CO, BC, Rn-222) and meteorological parameters (wind speed and direction, pressure, temperature, relative humidity) were also continuously monitored.

2.3 CCN measurements

The DMT CCN counter (Roberts and Nenes, 2005; Lance et al., 2006) is a cylindrical continuous-flow streamwise thermal gradient diffusion chamber. A constant streamwise temperature gradient is applied along the walls of the instrument flow chamber; the higher diffusivity of water vapor, relative to heat, results in supersaturation developing in the flow chamber. Before its introduction into the flow chamber, the sample is split into a "sheath" and a "aerosol" flow. The "sheath" flow is filtered and humidified before

ACPD
9, 10303–10336, 2009

its entry in the chamber, whereas the "aerosol" flow is introduced at the centerline of the flow and exposed to a constant supersaturation. The supersaturation is controlled by the chamber flow rate and the streamwise temperature gradient (Roberts and Nenes, 2005). The fraction of particles in the sample with S_c less than the instrument supersaturation activate into cloud droplets, are counted and sized upon exit from the flow tube in an Optical Particle Counter (OPC) using light from a 658 nm diode laser. A multichannel analyzer classifies the detected droplets into 20 size classes (from 0.75 to 10 μm diameter) and size distribution histograms are reported at 1 Hz frequency. Throughout the campaign, the instrument was operated at a total flow rate of 0.5 L min^{-1}, with a sheath-to-aerosol flow ratio of 10:1, and a top-bottom column difference, ΔT, between 4 and 15 K. Concentrations were measured at each supersaturation for 6 min, yielding a CCN spectrum every 30 min.

Calibration of the instrument supersaturation was done by determining the minimum diameter, D_p, of classified NaCl aerosol that activates at given chamber flow rate and ΔT. NaCl aerosol was generated by atomizing a sodium chloride aqueous solution (via a collision-type atomizer) and subsequently drying the droplet stream by passing it through two silica-gel diffusional driers (operating at ~5% RH). The resulting polydisperse dry aerosol was then charged using a Kr-85 neutralizer (TSI 3077A), and classified using a TSI 3080 Scanning Mobility Particle Sizer (SMPS) (consisted of a TSI 3010 condensation particle counter and a TSI 3081 differential mobility analyzer, DMA, operating under a sheath-to-aerosol ratio of 10:1). The classified aerosol flow was split and concurrently introduced into the CPC and the CCN instrument; the concentration of total particles (or, condensation nuclei, CN) and CCN were measured, and the activation fraction (CCN/CN) was computed. This process was repeated over many classified particle sizes (between 10 and 460 nm), so that an "activation curve" (i.e., CCN/CN as a function of mobility diameter) was obtained, which exhibits a characteristic sigmoidal shape. Figure 2a shows examples of activation curves obtained throughout the campaign (for a flow rate of 0.5 lpm and ΔT=15 K). The critical supersaturation of the particle with dry diameter, D_{p50}, at which half of the classified aerosol

activates (i.e., CCN/CN=0.5) is used to characterize the instrument supersaturation. Köhler theory (Eq. 2) is used to compute S_c from D_{p50}, assuming that the density of NaCl is equal to 2160 kg m^{-3} (CRC, 1993), surface tension of water and a molar mass of 0.058 kg mol^{-1}. The van't Hoff factor, v_s, was calculated as $v\Phi$, where v=2 are the moles of ions released into solution per mole of NaCl, and, Φ is the osmotic coefficient calculated by application of the Pitzer ion-interaction model (Pitzer and Mayorga, 1973) using interaction parameters provided by Clegg and Brimblecombe (1988). Φ is computed at the concentration corresponding to the CCN critical point (also computed from Köher theory; Padró et al., 2007). For the range of supersaturations considered in the calibrations (0.218 and 0.87%), v_s ranged between 1.91 and 1.87. This calibration procedure is repeated over a number of ΔT (Fig. 2b). The CCN instrument was calibrated numerous times throughout the campaign to characterize the stability of its characteristics.

2.4 Dry size distribution measurements

Prior to introduction into the SMPS, ambient aerosol was dried using two silica gel diffusional dryers, then charged by a Kr-85 neutralizer (TSI 3077A) and introduced into the DMA. The classified aerosol was then introduced into a TSI 3010 condensation particle counter (CPC) for measurements of particle concentration. The particle size distribution was obtained during a scan cycle (3 min) for mobility diameters between 20 and 460 nm. The sample flow rate in the DMA was set to 1 L min^{-1} and the sheath-to-aerosol flow ratio was maintained at 10:1.

2.5 Chemical composition

The aerosol chemical composition was determined by analysis of PTFE (PM_{10}, $PM_{1.3}$ and $PM_{1.3-10}$) and quartz (PM_1 and PM_{10}) filter samples (where aerosol was collected over 4 h). PTFE and quartz filters were analyzed for water-soluble ions after extraction with nanopure water. The solutions obtained were analyzed by ion chromatogra-

ACPD
9, 10303–10336, 2009

phy (IC) for anions (Cl^-, Br^-, NO_3^-, SO_4^{2-}, $C_2O_4^{2-}$) and cations (K^+, Na^+, NH_4^+, Mg^{2+}, Ca^{2+}), using the procedure of Bardouki et al. (2003). Quartz filters were also analyzed for organic and elemental carbon (Carbon Aerosol Analysis Lab Instrument, SUNSET Laboratory Inc.) and for water-soluble organic carbon (TOC-V_{CSH}, Total Organic Carbon Analyzer, SHIMATZU).

3 Results and discussion

3.1 CCN measurements

The time series of the total CN obtained from integration of the SMPS size distributions, and CCN measurements are shown in Fig. 3. The CCN generally correlate well with CN, with CCN concentrations increasing, as expected, with supersaturation. Throughout the measurement period, CCN concentrations at each supersaturation level varied by up to a factor of 3. The measured CCN concentrations at 0.60, 0.76 and 0.87% supersaturation were often very similar, suggesting that most particles activate at ~0.8%. The latter can be also derived from Fig. 4, where the activation fraction of the measured CCN versus total CN approaches unity at high supersaturations. This behavior is consistent with sampling aged aerosol, where particles are large in size and practically all contain significant amounts of soluble material.

The CCN concentration time series can be divided in five periods, based on the origin of the air masses sampled (Fig. 3). Period "A" represents the high CCN concentrations from air masses coming from the Balkans. The highest concentrations were observed on 25 September, during Period "B", when air masses originated from NE Europe. Period "C" was characterized by a decrease in CCN concentrations, consistent with the air masses originating from the "cleaner" south. As the wind direction shifted later on to westerly (Period "D"), the air originated from the Mediterranean and CCN concentrations were elevated. In the beginning of October (Period "E"), CCN concentrations were high (especially towards the end of the measurement campaign),

ACPD
9, 10303–10336, 2009

as air masses were coming from Asia Minor and NE Europe. The lowest CCN concentrations were observed on 22 September, after Period "A", as air originated from high in the free troposphere and descended into the marine boundary layer without passing near major aerosol sources. These results are summarized in Fig. 5a, showing the CCN concentrations grouped by prevailing wind direction.

The large scatter in measured activation fraction at each supersaturation (Fig. 4) is partially due to the air mass origin. This is shown clearly in Fig. 5b, which presents the measured CCN/CN separately for each wind direction. For the low supersaturations (0.22, 0.44%), CCN/CN is larger when the air masses are "cleaner" i.e. when they originated from the South (Fig. 5b). For the high supersaturations the ratio remains more or less constant (and close to unity, since most of the aerosol is activated) regardless of the air mass origin. As expected, the slope of the CCN spectrum is significant for N-NW airmasses, because of the presence of relatively small particles, a fraction of which remain unactivated even at high supersaturations.

3.2 Aerosol mass and composition measurements

The distinction between "polluted" (Fig. 1a, b) and "cleaner" (Fig 1c, d) air masses suggested from the back trajectories is reflected in the size distribution measurements (Fig. 6). Aerosol concentrations in air masses originating from central and northeastern Europe (21 and 25 September) were significantly higher (t-test, α=0.01) and with a larger number of smaller particles, than observed in air originating from the south (27 September). The corresponding average values (dN/dlogDp) for the aforementioned dates were 7804±929, 4119±386 and 3463±373. For particles smaller than 40 nm, the values were 897±178, 467±71 and 289±81, respectively.

The average particulate matter concentration during the measurement period was of 15.82±8.3 $\mu g\,m^{-3}$, with the PM_1 fraction accounting for 60.5±6.5% of the total mass. Ammonium sulfate accounted for up to 75% of the total inorganic mass fraction, with 79.8±6% of the total sulfate being in the fine mode. From the organic carbon analysis, the fine mode (PM_1) represented 74.8±12.3% of the total organic carbon concentra-

ACPD
9, 10303–10336, 2009

tion, varying from 0.6 to 4.1 $\mu g\,m^{-3}$. The similar $PM_1/PM_{2.5}$ ratios for organics and sulfate suggest that the aerosol is internally mixed, at least for aerosol above 1 μm. The WSOC analysis showed that 70% of the organic carbon was water-soluble, with this ratio remaining more or less constant throughout the whole measurement period. This ratio, though high, is expected for an area with aged aerosol (Jaffrezo et al., 2005 and references within). Finally, Fig. 7 shows the time series of the particulate organic matter and the ammonium sulfate loadings ($\mu g\,m^{-3}$) resulting from the compositional analysis, with an average of 8.6 $\mu g\,m^{-3}$ and 6.4 $\mu g\,m^{-3}$, respectively.

3.3 CCN closure

Before each closure calculation, the transients in the CCN instrument operation were screened to minimize observational biases. Each 6-min supersaturation segment was examined for (1) minimal fluctuations in the flow chamber temperature gradient and (2) stability of the flows. Fluctuations in temperature, if small enough, have a minimal impact on instrument supersaturation and closure (Ervens et al., 2007). If both criteria were satisfied, then the CCN concentrations were averaged over the last 2–3 min of each supersaturation segment and a closure calculation was done (Medina et al., 2007). SMPS size distributions were averaged over each supersaturation segment; only the scans overlapping with the CCN measurements were considered. The chemical composition for computing CCN properties was obtained from the analysis of the corresponding 4-h filters.

Most of the inorganic soluble fraction was ammonium sulfate ($greqs_{NH4}/greqs_{SO4}$ =0.93); other inorganic components (e.g. nitrate, chlorides, etc.) are neglected, as their concentration was very low throughout the measurement period. Thus, we assume the aerosol to be composed of a mixture of $(NH_4)_2SO_4$ and organics, and, the ammonium

ACPD
9, 10303–10336, 2009

sulfate volume fraction, ε_s can be calculated as

$$\varepsilon_s = \frac{\frac{m_s}{\rho_s}}{\frac{m_s}{\rho_s} + \frac{m_i}{\rho_i}} \quad (1)$$

where ρ_i, ρ_s is the density of the insoluble organic (1500 kg m^{-3}; Kostenidou et al., 2007) and $(NH_4)_2SO_4$ (1760 kg m^{-3}), respectively, and m_i, m_s are the mass loadings of organic and $(NH_4)_2SO_4$, respectively. For the measurement period, the volume fraction of ammonium sulfate had a mean value of 0.378±0.144. These values are consistent with long-term measurements at this site, where ammonium sulfate accounts for 46±10% of the total aerosol mass (84±8% of which is in the fine mode), and remains fairly constant throughout the year (Koulouri et al., 2008).

Based on the composition computed from Eq. (1), the critical supersaturation, Sc for each particle size d, is calculated from Köhler theory (e.g., Seinfeld and Pandis, 1998),

$$Sc = \left[\frac{256}{27}\left(\frac{M_w\sigma}{RT\rho_w}\right)^3\left(\frac{\rho_w}{M_w}\right)\left(\frac{M_s}{\rho_s}\varepsilon_s v_s + \frac{M_o}{\rho_o}\varepsilon_o v_o\right)^{-1} d^{-3}\right]^{1/2} \quad (2)$$

where R is the universal gas constant, T is the ambient temperature, σ is the surface tension of the CCN at the point of activation (assumed to be equal to that of water), M_s is the molar mass of the solute and M_w, ρ_w are the molar mass and density of water, respectively, computed at the average temperature of the CCN column. As done for NaCl calibration aerosol, the effective van't Hoff factor of the sulfate, v_s, is computed as $v\Phi$, where v=3 for $(NH_4)_2SO_4$, and Φ is computed from the Pitzer activity model (Pitzer, 1973), for the solute concentration at the critical point. M_o, ρ_o, ε_o, v_s in Eq. (2) are the molar mass, density, volume fraction and effective van't Hoff factor of the water-soluble organic fraction, respectively.

Predicting CCN concentrations for a closure study entails computing S_c for each aerosol size class in the measured size distributions, using the measured composition (Eq. 1). In applying Eq. (2), two cases are investigated: (a) assuming that the organic

ACPD
9, 10303–10336, 2009

fraction is insoluble, i.e., ε_o=0, and, (b) that 70% of the organics are water-soluble (as suggested by a carbon mass balance of extracted filters), i.e., ε_o=0.7(1−ε_s), where (1−ε_s) is the volume fraction of the organics in the particles. In reality, 70% organic solubility is an upper limit for the organic water-soluble fraction, since the amount of water mass available in recently activated CCN is usually much less than that used for WSOC filter extraction. In application of Eq. (2), we use ρ_o=1500 kg m^{-3} (Kostenidou et al., 2008) and M_o~200, consistent with values inferred from Köhler theory analysis of water-soluble organic samples collected from a variety of sources (Asa-Awuku et al., 2007, 2008, 2009; Engelhart et al., 2008).

Figure 8a shows the predicted against measured CCN for the whole measurement period, assuming that the organics are insoluble. On average, the closure is achieved to within 3.4±11%. For the lowest supersaturation (0.22%) there is an underprediction bias which is not seen at higher supersaturations (Table 1). The underprediction bias at low supersaturation is most likely due to neglecting the soluble organics in the calculations. Deviations of the measured bulk (PM_1) composition from that at CCN-relevant sizes (~100 nm at 0.2% supersaturation) is possible but not likely, because i) aerosol is internally mixed and composition does not vary between PM_1 and PM_{10} (i.e., 700 nm, 1.7 μm mobility diameter, respectively, assuming that the particles are spherical with a density of ~2000 kg m^{-3}; DeCarlo et al., 2004), ii) a remarkably constant single lognormal mode spans the 100–500 nm size range (Fig. 6), suggesting common production and ageing processes (i.e., chemical composition) for this size range, and, iii) long-term size resolved chemical composition of inorganic species and organic carbon in the area both show similar size-resolved composition variability, having one major peak at 0.346 μm (i.e., 240 nm mobility diameter) (Mihalopoulos, unpublished data).

If the organic water-soluble fraction is considered in the CCN calculations, the closure error on average is not affected much (+1.9±15% from −3.4±11% in Fig. 8a), but the underprediction bias at low supersaturations is substantially reduced (Fig. 8b). At high supersaturations however, closure worsens (Table 1), likely because the composi-

tion at small aerosol sizes (30–100 nm) deviates from the larger (∼100 nm and above) particles. The presence of a separate and variable ultrafine CCN mode (Fig. 6) suggests that indeed this is a plausible hypothesis. Assuming that the overprediction is solely from overestimation of the sulfate fraction (and that 70% of the organic remains soluble), a 10% reduction is required to account for this bias. Size-resolved aerosol composition measurements can confirm that this is indeed the case, and will be the focus of a future study.

3.4 Sensitivity of CCN closure to aerosol parameters

In this section, the sensitivity of CCN closure to aerosol properties assumed (i.e. organics density, and aerosol compositional measurement uncertainties) as well as the uncertainty in the gravimetric measurements (i.e. uncertainty in mass, volume fraction) is conducted. Generally it is observed that a 10% increase in the organic density improves the closure (+2%), and so does a 7% increase of the ammonium sulfate mass, which is even more apparent for the lowest supersaturation (+5%). The respective closure errors ($CCN_{predicted}$-$CCN_{measured}$ over $CCN_{measured}$) are −2.9±15 and −3.4±14%. Likewise, a 10% decrease in the organic density has a similar effect in the closure (−2%) as a 7% decrease of the ammonium sulfate mass, which is also more apparent for the lowest supersaturation. Overall, a ±10% change in the density of the organics results or a ±7% change in the ammonium sulfate mass, obtained from the experimental analysis, does not substantially affect the closure.

3.5 Droplet growth kinetics

Even though the soluble fraction (organic and inorganic) controls CCN activity, the insoluble organic fraction can also affect droplet formation by changing the uptake rate of water vapor onto growing droplets (e.g., Asa-Awuku, 2009). The OPC of the CCN counter provides information about the size of activated droplets as they exit the growth chamber, and, can be used to assess the impact of the organics on the uptake rate of

water vapor onto the growing CCN, using a method called "Threshold Droplet Growth Analysis" (TDGA). For this, droplet sizes from activated ambient CCN are compared to those of pure sodium chloride aerosol. Since NaCl (and other calibration aerosol salts, e.g., $(NH_4)_2SO_4$) is very hygroscopic, water vapor would meet little resistance during the uptake process and tend to grow as rapidly as possible, and provide a standard of "rapid growth" which ambient CCN can be compared against. Furthermore, we choose NaCl particles with S_c equal to the instrument supersaturation (i.e. a dry diameter of D_{p50}), so that the smallest possible size, D_{pmin} of activated droplet with rapid growth kinetics is determined. Activation of polydisperse ambient particles will exhibit a range of droplet sizes, but should all be larger than D_{pmin} over the range of supersaturations considered, if the water vapor uptake process is as fast as in NaCl. If the sizes of the droplets formed on ambient aerosol are statistically smaller than the sizes of those formed on pure NaCl aerosol, then the presence of organics do indeed delay the growth of the droplets; subsequent modeling of growth kinetic data could then express the delay in growth rate in terms of an effective uptake coefficient (e.g., Ruehl et al., 2008; Asa-Awuku et al., 2009).

Figure 11 presents application of TDGA to the droplet growth data for the whole measurement period. In agreement with theory (Lance et al., 2006) the droplet size augments as the supersaturation increases. The solid line represents the size of the activated calibration NaCl particles, with s_c equal to the instrument supersaturation, while the points represent the average droplet size from the ambient aerosol activation data. The variability in the droplet size seen in the NaCl data is of the same order as the OPC bin resolution (0.5 μm), and all the ambient droplet size data lie within this uncertainty. Hence, it can be concluded that on average, the very aged organics present in ambient aerosol in this area do not significantly delay the water uptake process. This is consistent with the biogenic SOA studies of Englehart et al. (2008) and Asa-Awuku et al. (2009), where strong kinetic limitations were observed only in situations where the water-soluble fraction of the aerosol was below 30%.

4 Summary and conclusions

Measurements of CCN from 0.22 to 0.87% supersaturation, aerosol size distribution and chemical composition were carried out at the Finokalia measuring site of the University of Crete, during the FAME-07 campaign (September–October, 2007). A variety of airmass types were sampled; polluted air coming from Europe tends to have higher concentrations of smaller particles and contains significant amounts of organic matter. Air masses from Asia Minor and North Africa tend to have lower particle concentrations, with larger CCN sizes, and, result in a higher activation fraction (CCN/CN). Organics sampled throughout the period were highly oxidized, as about 70% of the total organic mass was found to be water-soluble. Virtually all the particles activated at 0.8% supersaturation, consistent with the aged nature of the aerosol sampled.

Application of Köhler theory, using measurements of bulk composition and size distribution, resulted in excellent CCN closure. Assuming that organics are insoluble, closure was attained to within 3.4±11% for all supersaturations, with a tendency for underprediction (15±8%; r^2=0.92) at lower supersaturations (0.2–0.4%); this suggests that the water-soluble organic fraction contributes to the CCN activity. Indeed, including the effects of the water-soluble organic fraction improves the underprediction bias at low supersaturations, but introduces a slight overprediction (~5±15%) bias at higher supersaturations (0.6–0.8%), likely related to the size-dependant variations in sulfate content. Nevertheless, this study suggests that the error associated with application of the simplest form of Köhler theory (i.e., size-invariant composition, and insoluble organic fraction) results in relatively low closure error, notably less in fact than found for other locations close to large anthropogenic sources (e.g., Medina et al., 2007; Ervens et al., 2006). The maximum level of closure error, seen at low supersaturations (15±8%), when placed in the context of the aerosol indirect effect, results in about a 7±8% uncertainty in cloud droplet number (Sotiropoulou et al., 2006), and if representative of the globe, would result in roughly a 10–15% uncertainty in indirect forcing (Sotiropoulou et al., 2007).

ACPD
9, 10303–10336, 2009

Using threshold droplet growth analysis, the growth kinetics of ambient CCN is shown to be consistent with NaCl calibration aerosol. This suggests that the presence of aged organics does not seem to suppress the rate of water uptake on ambient CCN. This finding, if applicable to regions of the globe with very aged aerosol, suggests that water uptake processes in ambient particles should be described with the same kinetic parameters (i.e., uptake coefficient) as for pure inorganic salt particles. It should be noted however that all aerosol sampled during FAME-07 was residing in the humid boundary layer before sampling and may contain residual water; whether dry organic-rich particles residing in the free troposphere exhibit the same type of growth kinetic behavior (as suggested by Ruehl et al., 2008) is still unknown and is the objective of a future study.

Acknowledgements. A. Bougiatioti was supported by the Greek General Secretariat of Research and Technology, under PENED 2003 grant. A. Nenes acknowledges support from the US NSF (CAREER) and from NOAA-ACC. S. N. Pandis acknowledges support by the EU-CAARI European Union Project.

References

Albrecht, B. A.: Aerosols, cloud microphysics, and fractional cloudiness, Science, 245, 1227–1230, 1989.

Asa-Awuku, A., Engelhart, G. J., Lee, B. H., Pandis, S. N., and Nenes, A.: Relating CCN activity, volatility, and droplet growth kinetics of -caryophyllene secondary organic aerosol, Atmos. Chem. Phys., 9, 795–812, 2009, http://www.atmos-chem-phys.net/9/795/2009/.

Asa-Awuku, A., Sullivan, A. P., Hennigan, C. J., Weber, R. J., and Nenes, A.: Investigation of molar volume and surfactant characteristics of water-soluble organic compounds in biomass burning aerosol, Atmos. Chem. Phys., 8, 799–812, 2008, http://www.atmos-chem-phys.net/8/799/2008/.

Asa-Awuku, A., Nenes, A., Gao, S., Flagan, R. C., and Seinfeld, J. H.: Alkene ozonolysis SOA: inferences of composition and droplet growth kinetics from Köhler theory analysis, Atmos.

Chem. Phys. Discuss., 7, 8983–9011, 2007, http://www.atmos-chem-phys-discuss.net/7/8983/2007/.
Barahona, D. and Nenes, A.: Parameterization of cloud droplet formation in large-scale models: Including effects of entrainment, J. Geophys. Res.-Atmos., 112(D16), D16206, doi:10.1029/2007JD008473, 2007.
Bardouki, H., Liakakou, H., Economou, C., Sciare, J., Smolik, J., Zdimal, V., Eleftheriadis, K., Lazaridis, M., Dye, C., and Mihalopoulos, N.: Chemical composition of size-resolved atmospheric aerosols in the eastern Mediterranean during summer and winter, Atmos. Environ., 37, 195–208, 2003.
Brechtel, F. J. and Kreidenweis, S. M.: Predicting particle critical supersaturation from hygroscopic growth measurements in the humidified TDMA. Part 1: Theory and sensitivity studies, J. Aerosol Sci., 57, 1854–1871, 2000.
Broekhuizen, K., Chang, R.Y.-W., Leaitch, W. R., Li, S.-M., and Abbatt, J. P. D.: Closure between measured and modeled cloud condensation nuclei (CCN) using size-resolved aerosol compositions in downtown Toronto, Atmos. Chem. Phys., 6, 2513–2524, 2006, http://www.atmos-chem-phys.net/6/2513/2006/.
Cantrell, W. G., Shaw, G., Cass, G., Chowdhury, Z., Hughes, L., Prather, K., Guazzotti, S., and Coffee, K.: Closure between aerosol particles and cloud condensation nuclei at Kaashidhoo climate observatory, J. Geophys. Res., 106(D22), 28711–28718, 2001.
Chang, R. Y.-W., Liu, P. S. K., Leaitch, W. R., and Abbatt, J. P. D.: Comparison between measured and predicted CCN concentrations at Egbert, Ontario: Focus on the organic aerosol fraction at a semi-rural site, Atmos. Environ., 41, 8172–8182, 2007.
Charlson, R., Seinfeld, J., Nenes, A., Kulmala, M., Laaksonen, A., and Facchini, M.: Reshaping the theory of cloud formation, Science, 292, 2025–2026, 2001.
Covert, D., Gras, J., Wiedensholer, A., and Stratmann, F.: Comparison of directly measured CCN with CCN modeled from the number-size distribution in the marine boundary layer during ACE 1 at Cape Grim, Tasmania, J. Geophys. Res., 108(D21), 16597–16608, 1998.
Clegg, S. L. and Brimblecombe, P.: Equilibrium partial pressures of strong acids over concentrated saline solutions – I. HNO_3, Atmos. Environ., 22, 91–100, 1988.
CRC, Handbook of Chemistry and Physics, 74th Edition, CRC Press Inc., 1993.
Decesari, S., Facchini, M. C., Mircea, M., Cavalli, F., and Fuzzi, S.: Solubility properties of surfactants in atmospheric aerosol and cloud/fog water samples, J. Geophys. Res., 108(D21), 4685, doi:10.1029/ 2003JD003566, 2003.

Dusek, U., Covert, D., Wiedensholer, A., Neususs, C., Weise, D., and Cantrell, W.: Cloud condensation nuclei spectra derived from size distributions and hygroscopic properties of the aerosol in coastal southwest Portugal during ACE-2, Tellus, 55B, 35–53, 2003.

Engelhart, G. J., Asa-Awuku, A., Nenes, A., and Pandis, S. N.: CCN activity and droplet growth kinetics of fresh and aged monoterpene secondary organic aerosol, Atmos. Chem. Phys., 8, 3937–3949, 2008, http://www.atmos-chem-phys.net/8/3937/2008/.

Ervens, B., Cubison, M., Andrews, E., Feingold, G., Ogren, J. A., Jimenez, J. L., DeCarlo, P., and Nenes, A.: Prediction of cloud condensation nucleus number concentration using measurements of aerosol size distributions and composition and light scattering enhancement due to humidity, J. Geophys. Res., 112, D10S32, doi:10.1029/2006JD007426, 2007.

Facchini, M., Mircea, M., Fuzzi, S., and Charlson, R.: Cloud albedo enhancement by surface-active organic solutes in growing droplets, Nature, 401, 257–259, 1999.

Finlayson-Pitts, B. J. and Piits Jr., J. N.: Chemistry of the Upper and Lower Atmosphere: Theory, Experiments and Applications, Academic Press, San Diego, California, USA, 2000.

Fountoukis, C. and Nenes, A.: Continued development of a cloud droplet formation parameterization for global climate models, J. Geophys. Res., 110, D11212, doi:10.1029/2004JD005591, 2005.

Furutani, H., Dall'osto, M., Roberts, G. C., and Prather, K. A.: Assessment of the relative importance of atmospheric aging on CCN activity derived from field observations, Atmos. Environ., 42, 3130–3142, 2008.

Intergovernmental Panel on Climate Change, Climate Change 2007: Synthesis Report, 2007.

Jaffrezo, J.-L., Aymoz, G., Delaval, C., and Cozic, J.: Seasonal variations of the water soluble organic carbon mass fraction of aerosol in two valleys of the French Alps, Atmos. Chem. Phys., 5, 2809–2821, 2005, http://www.atmos-chem-phys.net/5/2809/2005/.

Ji, Q., Shaw, G., and Cantrell, W.: A new instrument for measuring cloud condensation nuclei: Cloud condensation nucleus "remover", J. Geophys. Res., 103, 28013–28019, 1998.

Köhler, H.: Zur condensation des wasserdampfe in der atmosphere, Geofys. Publ., 2, 3–15, 1921.

Köhler, H.: The nucleus in the growth of hygroscopic droplets, T. Faraday Soc., 32, 1152–1161, 1936.

Kostenidou, E., Pathak, R. K., and Pandis, S.: An algorithm for the calculation of secondary

organic aerosol density combining AMS and SMPS data, Aerosol. Sci. Tech., 41(11), 1002–1010, 2007.

Koulouri, E., Saarikoski, S., Theodosi, C., Markaki, Z., Gerasopoulos, E., Kouvarakis, G., Mäkelä, T., Hillamo, R., and Mihalopoulos, N.: Chemical composition and sources of fine and coarse particles in the Eastern Mediterranean, Atmos. Environ., 42, 6542–6550, 2008.

Lance, S., Medina, J., Smith, J., and Nenes, A.: Mapping the operation of the DMT continuous flow CCN counter, Aerosol Sci. Tech., 40, 242–254, 2006.

Lelieveld, J., Berresheim, H., Borrmann, S., Crutzen, P. J., Dentener, F. J., Fischer, H., Feichter, J., Flatau, P. J., Heland, J., Holzinger, R., Korrmann, R., Lawrence, M. G., Levin, Z., Markowicz, K. M., Mihalopoulos, N., Minikin, A., Ramanathan, V., De Reus, M., Roelofs, G. J., Scheeren, H. A., Sciare, J., Schlager, H., Schultz, M., Siegmund, P., Steil, B., Stephanou, E. G., Stier, P., Traub, M., Warneke, C., Williams, J., and Ziereis, H.: Global Air Pollution Crossroads over the Mediterranean, Science, 298, 794–799, 2002.

Liu, P., Leaitch, W., Banic, C., Li, S., Ngo, D., and Megaw, W.: Aerosol observations at Chebogue Point during the 1993 North Atlantic Regional Experiment: Relationships among cloud condnensation nuclei, size distribution and chemistry, J. Geophys. Res., 101, 28971–28990, 1996.

Medina, J., Nenes, A., Sotiropoulou, R.-E. P., Cottrell, L. D., Ziemba, L. D., Beckman, P. J., and Griffin, R. J.: Cloud condensation nuclei closure during the International Consortium for Atmospheric Research on Transport and Transformation 2004 campaign: Effects of size-resolved composition, J. Geophys. Res., 112, D10S31, doi:10.1029/2006JD007588, 2007.

Mihalopoulos, N., Stephanou, E., Kanakidou, M., Pilitsidis, S., and Bousquet, P.: Tropospheric aerosol ionic composition above the Eastern Mediterranean area, Tellus, 49B, 314–326, 1997.

Mircea, M., Facchini, M. C., Decesari, S., Cavalli, F., Emblico, L., Fuzzi, S., Vestin, A., Rissler, J., Swietlicki, E., Frank, G., Andreae, M. O., Maenhaut, W., Rudich, Y., and Artaxo, P.: Importance of the organic aerosol fraction for modeling aerosol hygroscopic growth and activation: a case study in the Amazon Basin, Atmos. Chem. Phys., 5, 3111–3126, 2005, http://www.atmos-chem-phys.net/5/3111/2005/.

Nenes, A. and Seinfeld, J. H.: Parameterization of cloud droplet formation in global climate models, J. Geophys. Res., 108, 4415, doi:10.1029/2002JD002911, 2003.

Nenes, A., Charlson, R. J., Facchini, M. C., Kulmala, M., Laaksonen, A., and Seinfeld, J. H.: Can chemical effects on cloud droplet number rival the first indirect effect?, Geophys. Res.

Lett., 29(17), 1848, doi:10.1029/2002GL015295, 2002.
Padró, L. T., Asa-Awuku, A., Morrison, R., and Nenes, A.: Inferring thermodynamic properties from CCN activation experiments: single-component and binary aerosols, Atmos. Chem. Phys., 7, 5263–5274, 2007, http://www.atmos-chem-phys.net/7/5263/2007/.
Pitzer, K. S.: Thermodynamics of electrolytes. I. Theoretical Basis and general equations, J. Phys. Chem., 77, 268–277, 1973.
Pitzer K. S. and Mayorga, G.: Thermodynamics of electrolytes. II. Activity and osmotic coefficients for strong electrolytes with one or both ions univalent, J. Phys. Chem., 77, 2300–2308, 1973.
Reade, L., Jennings, S. G., and McSweeney, G.: Cloud condensation nuclei measurements at Mace Head, Ireland, over a period 1994–2002, Atmos. Res., 82, 610–621, 2006.
Rissman, T. A., VanReken, T. M., Wang, J., Gasparini, R., Collins, D. R., Jonsson, H. H., Brechtel, F. J., Flagan, R. C., and Seinfeld, J. H.: Characterization of ambient aerosol from measurements of cloud condensation nuclei during the 2003 atmospheric radiation measurement aerosol intensive observational period at the Southern Great Plains site in Oklahoma, J. Geophys. Res., 111, D05S11/1–D05S11/20, 2006.
Roberts, G. C., Nenes, A., Seinfeld, J. H., and Andreae, M. O.: Impact of biomass burning on cloud properties in the Amazon Basin, J. Geophys. Res, 108(D2), 4062, doi:10.1029/2001JD000985, 2003.
Roberts, G. and Nenes, A.: A continuous-flow streamwise thermal-gradient CCN chamber for atmospheric measurements, Aerosol Sci. Tech., 39, 206–221, 2005.
Roberts, G. C., Mauger, G., Hadley, O., and Ramanathan, V.: North American and Asian aerosols over the Eastern Pacific Ocean and their role in regulating cloud condensation nuclei, J. Geophys. Res., 111, D13205, doi:10.1029/2005JD006661, 2006.
Ruehl, C. R., Chuang, P. Y., and Nenes, A.: How quickly do cloud droplets form on atmospheric particles?, Atmos. Chem. Phys., 8, 1043–1055, 2008, http://www.atmos-chem-phys.net/8/1043/2008/.
Seinfeld, J. and Pandis, S.: Atmospheric Chemistry and Physics: From Air Pollution to Climate Change, John Wiley, Hoboken, NJ, USA, 1998.
Sciare, J., Oikonomou, K., Cachier, H., Mihalopoulos, N., Andreae, M. O., Maenhaut, W., and Sarda-Estéve, R.: Aerosol mass closure and reconstruction of the light scattering coefficient over the Eastern Mediterranean Sea during the MINOS campaign, Atmos. Chem. Phys., 5,

2253–2265, 2005,
http://www.atmos-chem-phys.net/5/2253/2005/.
Shulman, M., Jacobson, M., Charlson, R., Synovec, R., and Young, T.: Dissolution behavior and surface tension effects of organic compounds in nucleating cloud droplets, Geophys. Res. Lett., 23, 277–280, 1996.
Snider, J., Guibert, S., Brenguier, J., and Putaud, J.: Aerosol activation in marine stratocumulus clouds: 2. Köhler and parcel theory closures studies, J. Geophys. Res., 108(D15), 8629, doi:10.1029/2002JD002692, 2003.
Sotiropoulou, R. E. P, Nenes, A., Adams, P. J., and Seinfeld, J. H.: Cloud condensation nuclei prediction error from application of Kohler theory: Importance for the aerosol indirect effect, J. Geophys. Res., 112, D12202, doi:10.1029/2006JD007834, 2007.
Sotiropoulou, R. E. P, Medina, J., and Nenes A.: CCN predictions: is theory sufficient for assessments of the indirect effect?, Geophys. Res. Lett., 33, L05816, doi:10.1029/2005GL025148, 2006.
Stroud, C. A., Nenes, A., Jimenez, J. L., DeCarlo, P. F., Huffman, J. A., Bruintjes, R., Nemitz, E., Delia, A. E., Toohey, D. W., Guenther, A. B., and Nandi, S.: Cloud activating properties of aerosol observed during CELTIC, J. Atmos. Sci., 64, 441–459, 2006.
Twomey, S.: The influence of pollution on the shortwave albedo of clouds, J. Atmos. Sci., 34, 1149–1152, 1977.
VanReken, T. M., Rissman, T. A., Roberts, G. C., Varutbangkul, V., Jonsson, H. H., Flagan, R. C., and Seinfeld, J. H.: Toward aerosol/cloud condensation nuclei (CCN) closure during CRYSTAL-FACE, J. Geophys. Res., 108(D20), 4633, doi:10.1029/2003JD003582, 2003.
Vrekoussis, M., Liakakou, E., Koçak, M., Kubilay, N., Oikonomou, K., Sciare, J., and Mihalopoulos, N.: Seasonal variability of optical properties of aerosols in the Eastern Mediterranean, Atmos. Environ., 39, 37, 7083–7094, 2005.

Table 1. Regression statistics for the CCN closure.

Supersaturation (%) (data points)	WSOC/OC=0 $\frac{CCN_{predicted}}{CCN_{observed}}$	WSOC/OC=0 R^2	WSOC/OC=0.7 $\frac{CCN_{predicted}}{CCN_{observed}}$	WSOC/OC=0.7 R^2
0.22 (261)	0.85	0.92	0.98	0.89
0.44 (265)	0.97	0.91	1.07	0.87
0.60 (265)	0.99	0.91	1.07	0.87
0.76 (265)	1.01	0.91	1.07	0.87
0.87 (266)	0.98	0.88	1.04	0.87

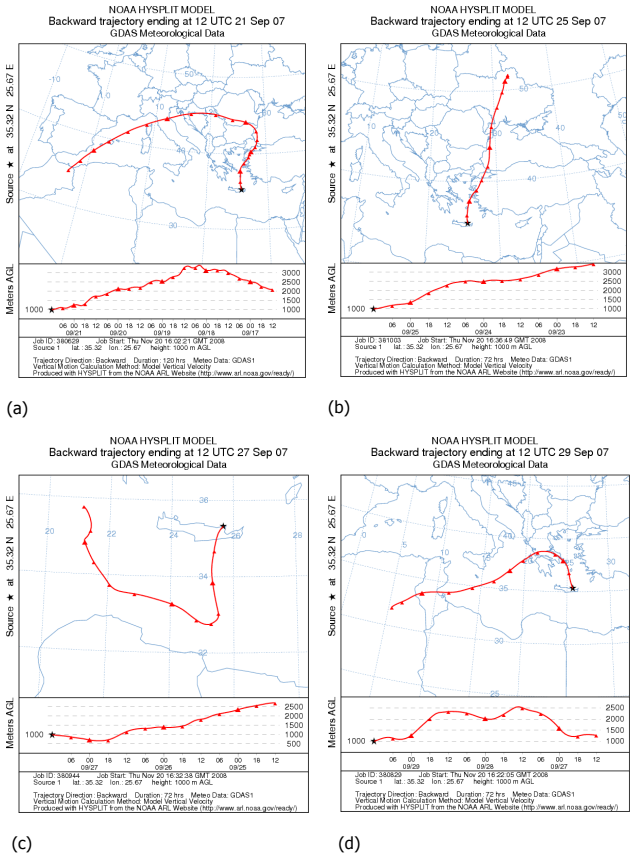

Fig. 1. Maps indicating the location of the sampling site and three-day HYSPLIT back trajectories for characteristic types of air masses sampled during FAME-07: **(a)** 21 September 2007 (Period "A"), **(b)** 25 September 2007 (Period "B"), **(c)** 27 September 2007 (Period "C"), and **(d)** 29 September 2007 (Period "D").

ACPD
9, 10303–10336, 2009

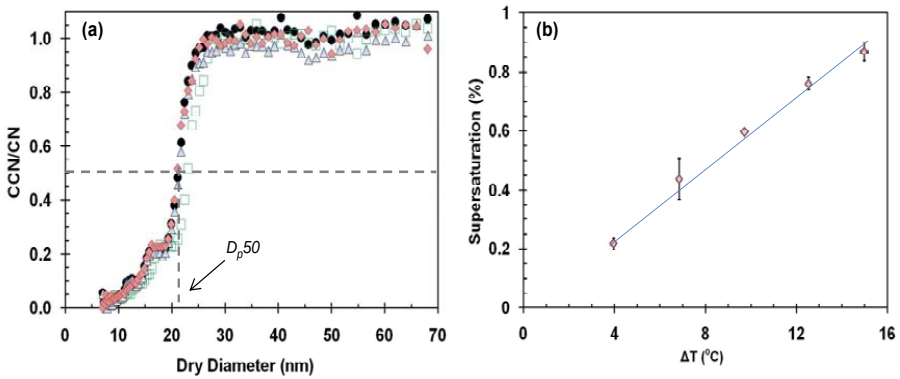

Fig. 2. **(a)** Activation curves for NaCl calibration aerosol, obtained for a top-bottom column temperature difference $\Delta T = 15$ K. **(b)** Instrument supersaturation versus ΔT.

ACPD
9, 10303–10336, 2009

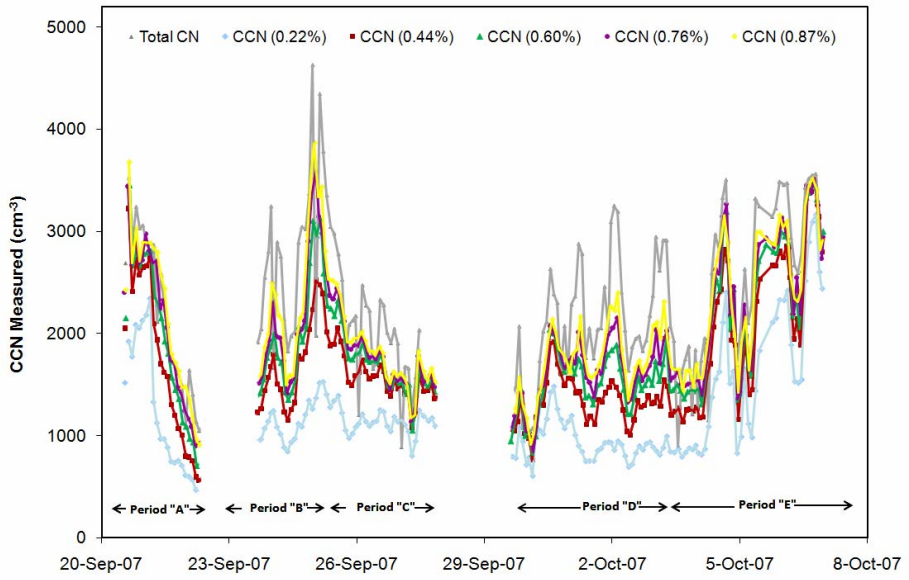

Fig. 3. Time series of the CN and CCN measurements throughout the measurement period.

ACPD
9, 10303–10336, 2009

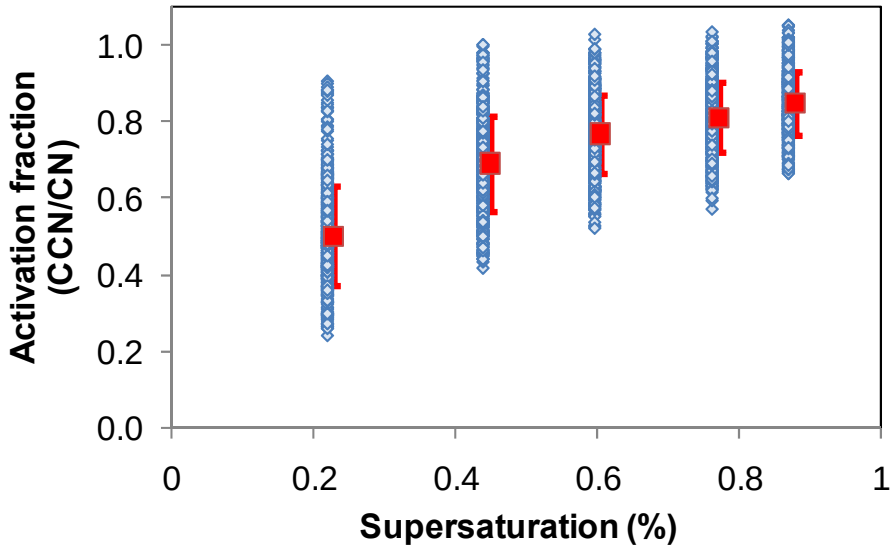

Fig. 4. Measured activation fraction versus supersaturation for the ambient aerosol, with the mean value and standard deviation from mean marked with red.

ACPD
9, 10303–10336, 2009

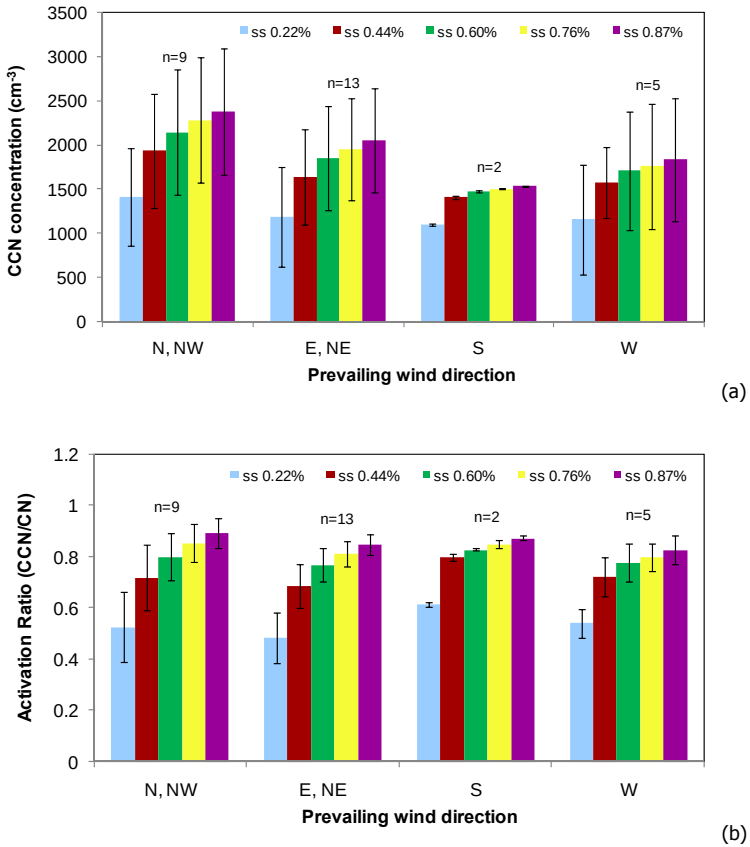

Fig. 5. (a) CCN average concentrations and corresponding standard deviations, and, **(b)** activation fraction and corresponding standard deviation for each prevailing wind direction, *n* being the number of 12-h periods where the wind direction was constant.

ACPD
9, 10303–10336, 2009

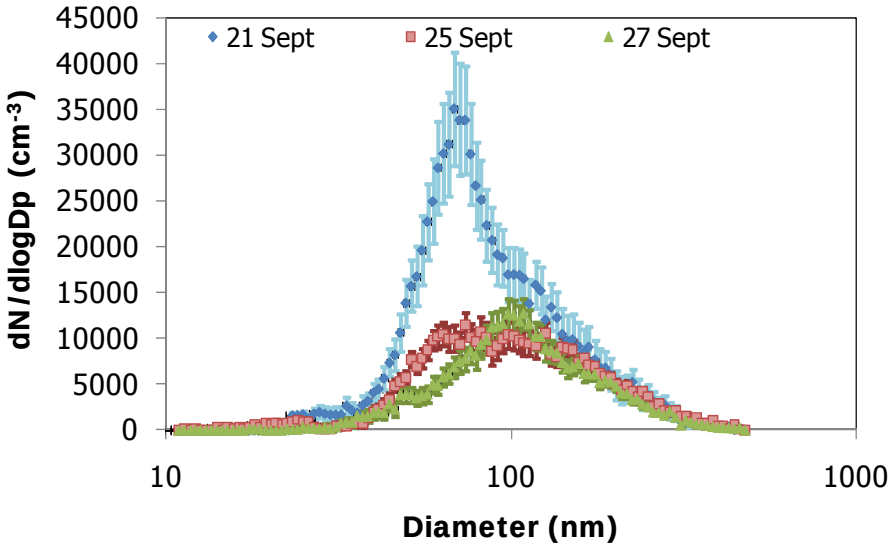

Fig. 6. Daily average aerosol size distributions, characteristic of the air masses sampled.

ACPD
9, 10303–10336, 2009

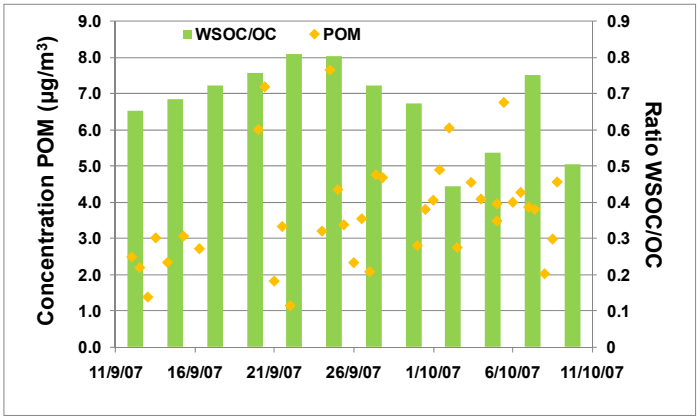

(a)

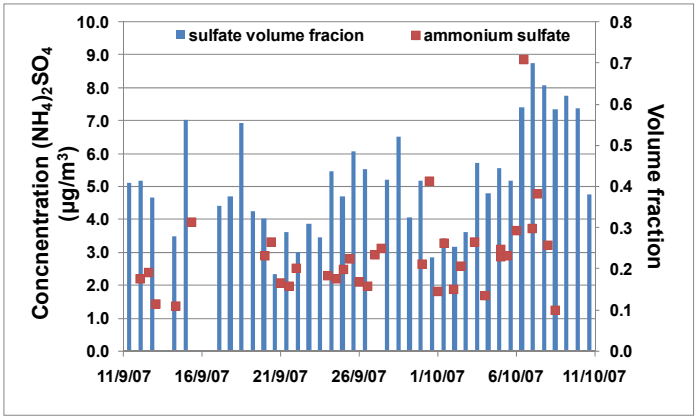

(b)

Fig. 7. Time series of **(a)** the particulate organic matter (PM_{10}) and WSOC/OC ratio and **(b)** the ammonium sulfate concentration (PM_{10}) and the sulfate volume fraction.

ACPD
9, 10303–10336, 2009

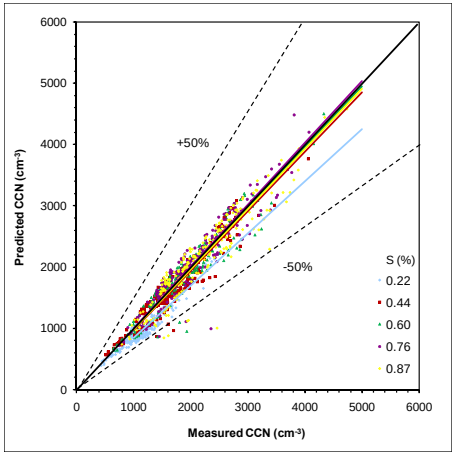

(a)

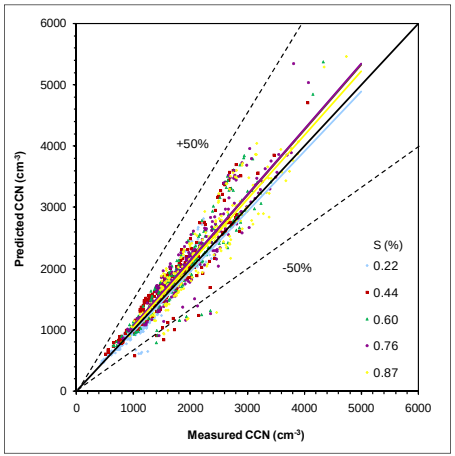

(b)

Fig. 8. Calculated versus measured CCN concentrations; **(a)** without and **(b)** with considering 70% of organics to be water-soluble.

ACPD
9, 10303–10336, 2009

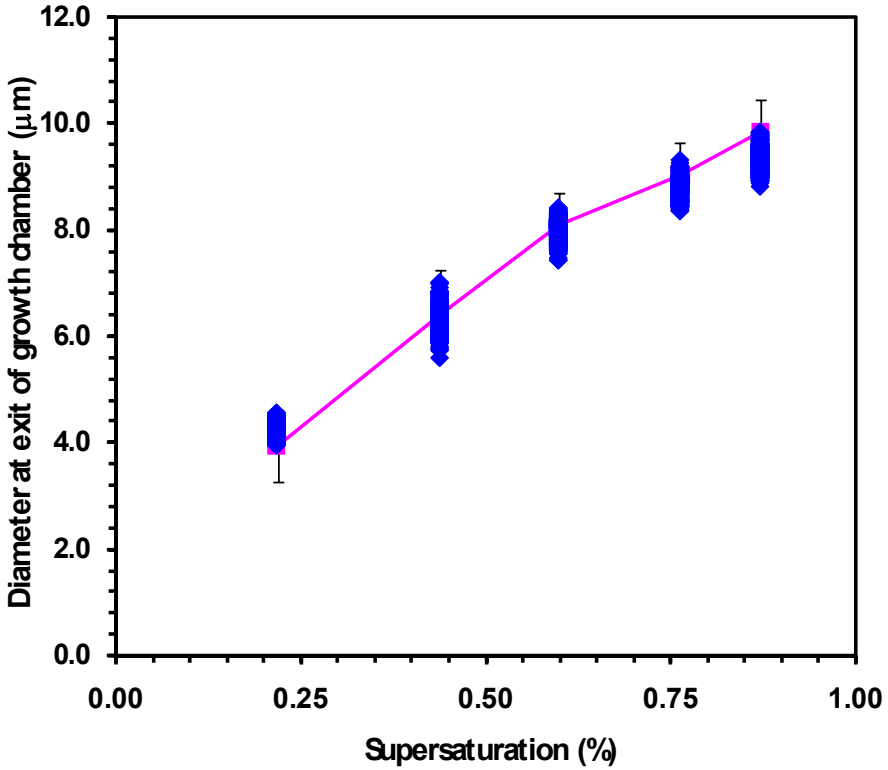

Fig. 9. Droplet sizes of CCN at the different supersaturations.